JTTEE5 5:298-302

Characteristics of High Hardness Alumina Coatings Formed by Gas Tunnel Plasma Spraying

A. Kobayashi

High hardness alumina coatings were formed at atmospheric pressure by gas tunnel plasma spraying, and the characteristics of these coatings were investigated. The hardness on the cross section of the alumina coating at a short spraying distance was more than 1300 HV, and the thickness of the hard layer increased with an increase of power input. The microstructure of the alumina coating was investigated by microscopy and x-ray diffraction (XRD) methods. It was ascertained that the cell size was small (~10 μm), and α-alumina was dominant in the high hardness layer of the coating. Finally, the effect of plasma energy was estimated from these results.

Keywords α-alumina, alumina coating, gas tunnel plasma spraying, high hardness coating, high hardness layer, microstructure, polarizing microscope, Vickers hardness

1. Introduction

PLASMA SPRAYED ceramic coatings exhibit porosity (Ref 1), which diminishes the mechanical and chemical properties of the coating and limits its practical application. Gas tunnel type plasma spraying was developed (Ref 2) to mitigate such characteristics (Ref 3-5).

Study of the deposit characteristics of gas tunnel spraying (Ref 4) indicated that the sprayed particles are in a fully molten state on contact with the substrate. As a result, the porosity is decreased, and mechanical properties, such as Vickers hardness, are improved. Therefore, a higher quality ceramic coating can be obtained by the gas tunnel plasma spraying method than with conventional plasma spraying.

New functional materials have been produced by plasma spraying with potential in numerous technological applications (Ref 6, 7). For example, high quality coatings of alumina with a Vickers hardness of 1200 to 1600 HV have been obtained by gas tunnel plasma spraying (Ref 8).

In this study, an alumina coating was formed by gas tunnel plasma spraying at a short spray distance, and the coating characteristics were investigated. The Vickers hardness of the cross section was measured for this alumina coating, and the effect of the spraying conditions (spraying distance, power input, etc.) on the properties of the alumina coating were investigated.

The microstructure of an obtained alumina coating was investigated by optical microscopy including a polarizing microscope (Ref 9). In addition, the crystal form of alumina on the surface was investigated by XRD; the relation to Vickers hardness was discussed.

2. Experimental

The gas tunnel plasma spraying apparatus used in this study is shown in Fig. 1. Its mechanism and properties were described in Ref 2 to 4.

A. Kobayashi, Joining and Welding Research Institute, Osaka University, Ibaraki, Osaka 567, Japan.

Figure 1 shows a plasma torch that is similar in structure and properties to a conventional plasma torch, A, and a gas tunnel plasma torch, B, that consists of a vortex generator, an inside nozzle electrode, and an outside nozzle electrode (gas divertor nozzle). The distance between the two electrodes was 46 mm, and the diameter of the gas divertor nozzle was 12 mm.

The experiment to form ceramic coatings was carried out at atmospheric pressure using a gas tunnel plasma jet with argon working gas. The distance between the torch and the substrate is the spraying distance, L, and a coating was formed by scanning the substrate in front of the torch. Table 1 shows the experimental conditions for the alumina coating.

Table 1 Experimental conditions

Power input (P), kW	20-30
Working gas (Ar) flow rate (Q), L/min	200
Powder feed rate (w), g/min	80
Spray distance (L), mm	20-80
Traverse speed (v), m/min	2.8

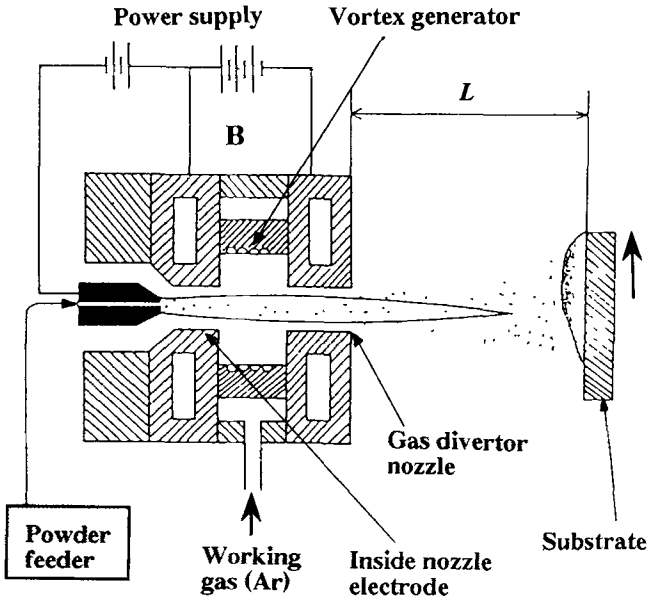

Fig. 1 Schematic diagram of the gas tunnel plasma spraying apparatus. A is conventional plasma torch. B is gas tunnel plasma torch. L is spraying distance.

An alumina powder of 99.5 wt% Al_2O_3 of size 10 to 40 μm was used in this study. A commercially available SUS304 plate (25 by 50 by 5 mm) was used as a substrate. The surface of the substrate was shot blasted prior to spraying.

The Vickers hardness, HV, was measured at the cross section of coatings formed under various spraying conditions. The following Vickers hardness conditions were used. The loading weight was 300 g. The holding time was more than 15 s, and at least 10 measurements were carried out at each location. The coating hardness was decided by the average value of the top part of the coating.

Generally speaking, the alumina coating consists of γ-alumina with some α-alumina (Ref 10). As a crystal system, α-alumina has a hexagonal lattice and optical anisotropy, which is observed as a bright color (white) under a microscope in a cross polarizing condition. On the other hand, γ-alumina has a cubic lattice and optical isotropy, which appears as a dark color (black) under a polarizing microscope (Ref 11). This observation was confirmed by XRD. The α-alumina concentration increased with the brightness of the coating in the polarizing microscope. In this way, the ratio of α-alumina on the surface was determined by the brightness of the image using the polarizing microscope.

3. Results

3.1 *Formation of the High Hardness Alumina Coating*

Figure 2 shows the dependency of the Vickers hardness of the cross section of an alumina coating produced by gas tunnel plasma spraying with respect to the spray distance, L.

Spalling appeared between the sprayed coating and the substrate at a distance, L, shorter than 20 mm when power input, P, was 30 kW. The spalling of the coating was effectively suppressed under the other spray conditions used in this experiment. The Vickers hardness increased with decreasing spray distance as shown in Fig. 2. The increase rate is greater at a spray distance less than L_p. Here, L_p is a critical spray distance at which the characteristics of the Vickers hardness change significantly.

The characteristics of the Vickers hardness are similar in power input, P of 20 and 30 kW. However, with a larger power input, a greater hardness could be obtained at each spray distance, and consequently, L_p increased. The greatest hardness, HV, of the alumina coating is 1500 at a spraying distance of 30 mm when power input is 30 kW.

In this manner, an extremely high hardness alumina coating can be obtained by gas tunnel plasma spraying at a short spray distance ($L < L_p$). It is difficult to produce such a high hardness alumina coating under conventional plasma spraying methods. The usual hardness of these coatings is 800 to 900 HV.

The effect of plasma energy, as determined by the length of the plasma jet, l_p, on the critical spraying distance, L_p, was measured from a photograph of the plasma jet. Figure 3 shows both lengths of l_p and L_p for power inputs of 20 and 30 kW.

As the power input is increased, the plasma length, l_p, becomes longer from 28 to 32 mm, and as a result, the L_p value increases in the short distance spraying region A shown in Fig. 3. It was found that L_p is about 10 mm longer than l_p at each power input. The coating surface temperature is almost the same at each L_p. Therefore, the plasma length, l_p, has a strong effect on the hardness of the coating surface.

3.2 *Distribution of Vickers Hardness*

Figure 4 shows the distribution of the hardness with respect to the coating cross section. The measurement was carried out at each distance from the coating surface in the thickness direction. The coating thickness was about 450 μm. In this case, the power input was 20 kW, the spraying distance was 30 mm, and the other spraying conditions were the same as for Fig. 2.

The distribution of the Vickers hardness shows a parabolic curve; that is, the Vickers hardness for the coating near the surface ($l = 0$) is higher than that near the substrate. The peak hardness is >1300 HV at ~200 μm l from the coating surface.

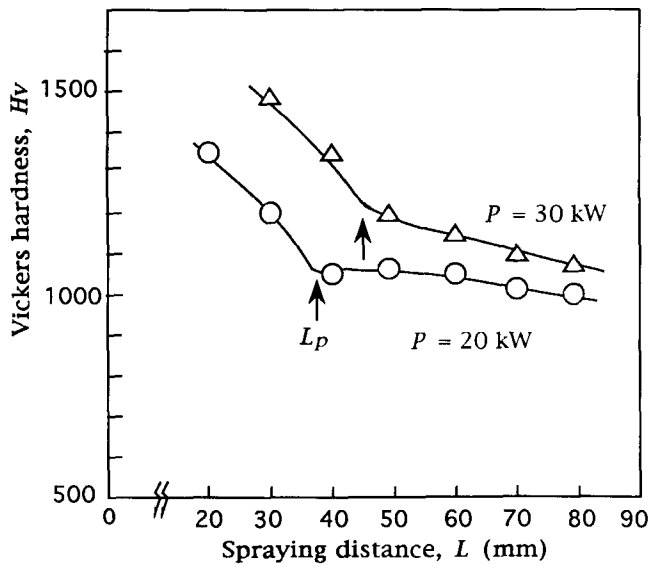

Fig. 2 Dependency of Vickers hardness of alumina coating on spraying distance at 20 and 30 kW P. L_p is critical spraying distance.

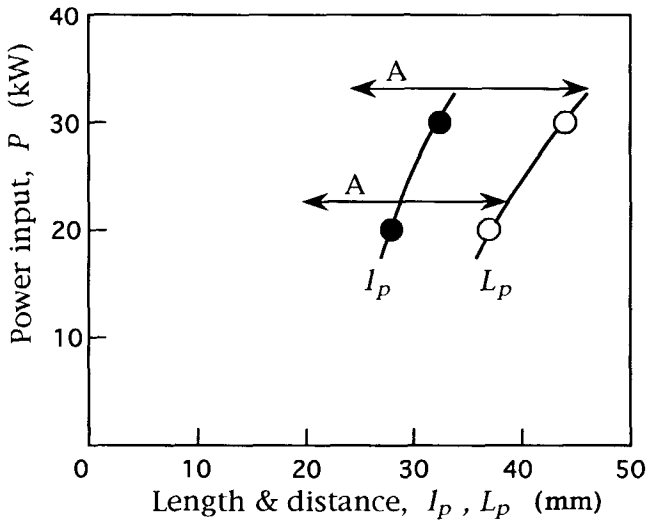

Fig. 3 Plasma length, l_p, and critical spraying distance, L_p, at 20 and 30 kW P. A is short distance spraying region.

On the other hand, an alumina coating formed at the usual spraying distance, $L > L_p$, exhibited a flat distribution of Vickers hardness on the cross section in the thickness direction; that is, there is no extremely high hardness region in the coating.

Figure 5 shows the hardness distribution in the case of high power input, P of 30 kW. In this case, the other spraying conditions were the same as for Fig. 4, and the coating thickness was also about 450 μm. This distribution also takes the shape of a parabolic curve. However, the coating hardness near the surface is much higher than that at 20 kW P while the hardness value near the substrate is a similar value for both power inputs. The high hardness region (>1300 HV) of the surface side is broader than that at 20 kW P. As well, the peak hardness shifted closer to the surface (150 l) where there is a high value of 1600 HV.

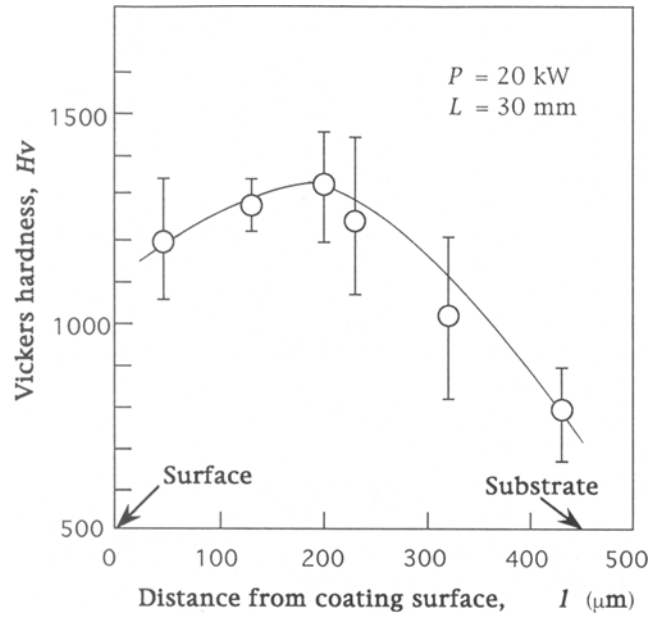

Fig. 4 Distribution of the Vickers hardness on the cross section of the alumina coating in the thickness direction

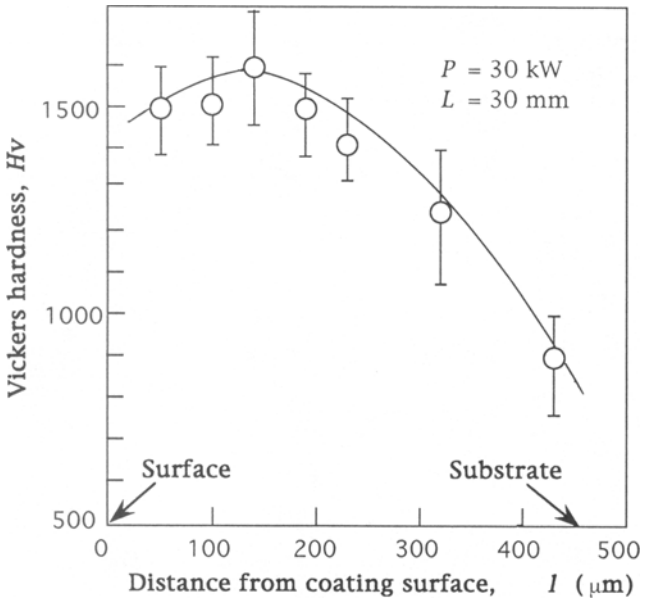

Fig. 5 Distribution of the Vickers hardness on the cross section of the alumina coating in the thickness direction in the case of large power input

3.3 *Microstructure of the High Hardness Alumina Coating*

The microstructure of the high hardness alumina coating was examined by microscopy. Figure 6 shows the alumina coating cross section. This coating is the same as that tested for Fig. 4 and was formed with three torch traverses under the conditions of 20 kW P and 30 mm L. Examination of the cross section (where the coating thickness is about 450 μm) shows that there are differences in the coating microstructure; see A, B, and C in Fig. 6.

Regions A and B correspond to the high hardness region in Fig. 4, in which the distance from the surface is less than 300 μm and the Vickers hardness is more than 1000 HV. This coating region was formed during the second and third passes of the torch.

In part B, the cell size is small compared to the other regions and forms a layer that is ~60 μm thick, which corresponds to the area >1300 HV shown in Fig. 4. On the other hand, for region A near the coating surface, the cell size is greater. In this region, the hardness is a little lower than that in area B.

Closest to the substrate, region C corresponds to the first torch pass. This part has the same coating structure as that formed by gas tunnel plasma spraying at the usual spraying distance. Figure 7 shows the coating cross section under a polarizing microscope for the same coating as that examined in Fig. 6.

Region C is formed during the first traverse and consists of an upper dark layer that is γ-alumina rich and a lower layer near the substrate that is a bright, α-alumina rich area. The brightness in-

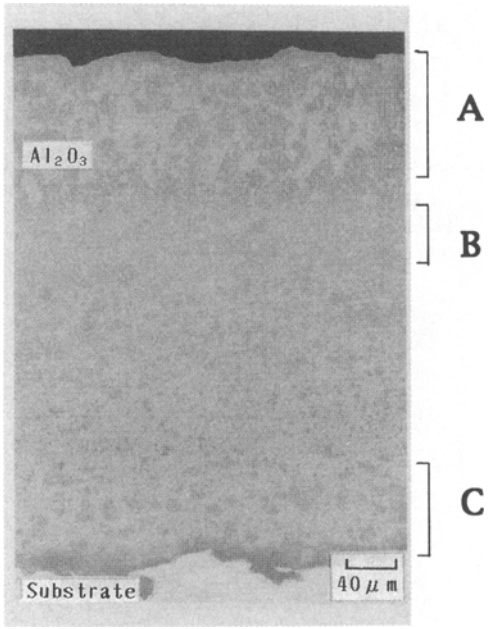

Fig. 6 Photograph of the cross section of high hardness alumina coating shown in Fig. 4. The thickness of this coating is about 450 μm for 20 kW P and 30 mm L.

creases considerably on the coating over region C. Region B has a fine structure and is the brightest indicating that this layer has a high concentration of α-alumina.

Region A, near the surface and formed on the third pass of the torch, has the highest brightness and indicates a high concentration of α-alumina. Regions under A are slightly darker and indicate a mixture of α-alumina and γ-alumina phases.

The alumina coating, which was formed at the usual spraying distance, L of 80 mm ($>L_p$) when power input, P, was 20 kW, has a uniform brightness over all the cross section. Therefore, the ratio of α-alumina and γ-alumina is nearly constant for the whole coating, which corresponds to the flat distribution of the Vickers hardness in the thickness direction.

4. Discussion

Figure 8 illustrates the relation between the structure and the properties of the coating, that is, the distributions of hardness for the condition of 20 kW P and 30 mm L.

As shown in this figure, region B, which has a hardness of more than 1300 HV, is called a "high hardness layer." This sublayer is about 60 μm thick and appears in the middle of the coating thickness. The cell size is very small in this region compared to the other regions. Region B is α-alumina rich.

In addition, the surface temperature during spraying was very high for the above-mentioned plasma energy. Table 2 shows the maximum temperature of the coating surface and the cooling rate of the surface. The maximum temperature is 1870 K at 50 mm L, which is near the melting point of alumina, 2110 K. The cooling rate also increases due to the high temperature. According to these results, it is assumed that the surface temperature exceeds the melting point at a shorter spraying distance.

Table 2 Maximum temperature and cooling rate on coating surface at 20 kW P

Spray distance (L), mm	50	80
Maximum temperature, K	1873	1273
Cooling rate, K/s	400	340

The formation of the high hardness layer is explained. At short spraying distance, the alumina coating is affected by the large plasma energy, and the surface of deposited particles is remelted. Consequently, the crystal form changes from γ-alumina to α-alumina, and the high cooling rate at high temperature causes the fine structure in layer B as shown in Fig. 6. In the surface layer, on the other hand, the cooling rate is estimated to be less than that in layer B: the inside of the coating, which leads to a larger cell size in layer A.

The case of a large power input of 30 kW is shown in Fig. 5. This coating also exhibits layer C, however, where the high hardness layer B becomes much thicker (300 μm) than that for 20 kW P. Here, the microstructure is fine and α-alumina rich. This layer broadens to the surface without region A, which appears in Fig. 6.

5. Conclusions

The high hardness alumina coating formed by gas tunnel plasma spraying was investigated, and the following results were obtained.

The Vickers hardness of the alumina coating increased with a decrease in the spraying distance and achieved a very high value at a short spraying distance of $L < L_p$. The critical spraying distance was directly related to the plasma length. A typical coating, for which the thickness was 450 μm and the hardness was 1500 HV (maximum is 1600 HV), was obtained under conditions of 30 kW P and 30 mm L.

The hardness distribution of the coating (in the thickness direction) has a parabolic profile, and the surface side of the coat-

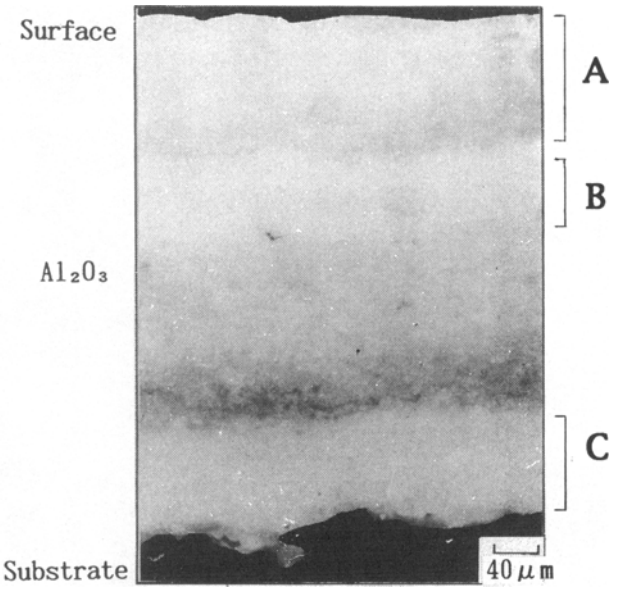

Fig. 7 Photograph of the same alumina coating shown in Fig. 6 under a polarizing microscope for 20 kW P and 30 mm L

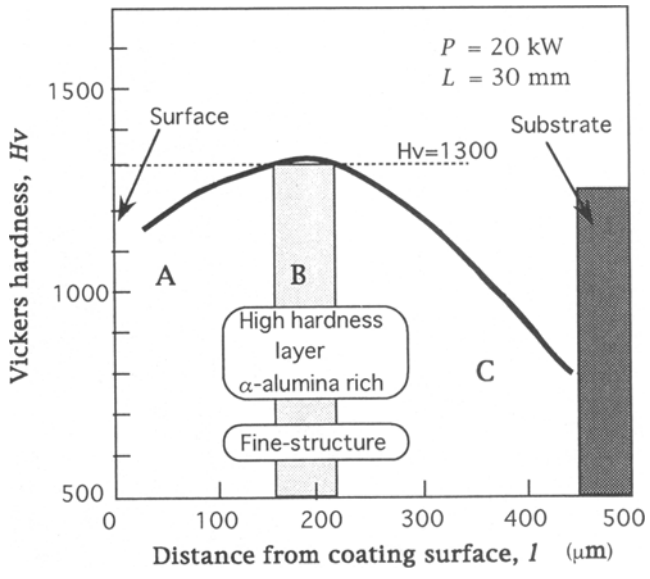

Fig. 8 Vickers hardness on the cross section of alumina coating shown in Fig. 4 and the relation to microstructure for 20 kW P and 30 mm L

ing was harder than the layer near the substrate. The coating hardness increased as the power input was increased, and the thickness of the high hardness layer increased.

The coating microstructure revealed that the structure was dense and that the cell size near the surface was very small (which corresponds to high hardness in that region of the coating). The coating surface was strongly influenced by the plasma energy.

The crystal form of alumina was distinguishable with a reflecting type polarizing microscope. The high hardness layer corresponded to the α-alumina rich layer.

Acknowledgments

The author thanks Mr. N. Hasegawa for his help during the experiment. This study was financially supported in part by a Grant-in-Aid for Scientific Research from the Japanese Ministry of Education, Science and Culture.

References

1. *Thermal Spraying Handbook,* Jpn. Inst. Thermal Spraying, Shin-gijutsu Kaihatsu Center, 1987 (in Japanese)
2. Y Arata, A. Kobayashi, and Y. Habara, Ceramic Coatings Produced by Means of a Gas Tunnel Type Plasma Jet, *J. Appl. Phys.,* Vol 62 (No. 12), 1987, p 4884-4889
3. Y. Arata, A. Kobayashi, and Y. Habara, Formation of Alumina Coating by Gas Tunnel Type Plasma Spraying Apparatus, *J. High Temp. Soc.,* Vol 13 (No. 3), 1987, p 116-124 (in Japanese)
4. A. Kobayashi, S. Kurihara, Y. Habara, and Y. Arata, Deposit Characteristic of Sprayed Powder and Ceramic Coating Characteristic Formed by Gas Tunnel Type Plasma Spraying, *Q. J. Jpn. Weld. Soc.,* Vol 8 (No. 4), 1990, p 457-463 (in Japanese)
5. Y. Arata, A. Kobayashi, and S. Kurihara, Effect of Spraying Conditions in Gas Tunnel Type Plasma Spraying, *J. High Temp. Soc.,* Vol 15 (No. 5), 1989, p 210-216 (in Japanese)
6. J. Hasui, *J. Weld. Soc. Jpn.,* Vol 37 (No. 4), 1987, p 52-58
7. A. Kobayashi, New Applied Technology of Plasma Heat Source, *Weld. Int.,* Vol 4 (No. 4), 1990, p 276-282
8. A. Kobayashi, Y. Habara, and Y. Arata, Structure of Alumina Coating Produced by Gas Tunnel Type Plasma Spraying, *J. High Temp. Soc.,* Vol 18 (No. 2), 1992, p 89-96 (in Japanese)
9. *Crystal Optics,* Jpn. Soc. Appl. Phys. Morikita Shuppan, 1975 (in Japanese)
10 N. Iwamoto, N. Umesaki, et al., Bond Adhesion of Plasma-Sprayed Alumina Coatings and The Effect of Pretreatments of Metals on Adhesive Strength, *J. High Temp. Soc.,* Vol 12 (No. 3), 1986, p 130-136 (in Japanese)
11. Y. Horie, Development of Functionality Materials by Plasma Spraying, *Kinzoku,* No. 8, 1988, p 71-75 (in Japanese)